

Original Research Article

<https://doi.org/10.20546/ijcmas.2020.911.109>

## Removal of Diclosulam Pesticide Residues in Water samples using Cu Doped ZnO Nanocatalyst

Varada Nageswara Rao<sup>1</sup>, N. V. S. Venu Gopal<sup>2\*</sup> and T. B. Patrudu<sup>3</sup>

<sup>1</sup>Department of Chemistry, Acharya Nagarjuna University, Guntur, Andhra Pradesh, India

<sup>2</sup>Department of Chemistry, Institute of Science, GITAM University, Visakhapatnam, India

<sup>3</sup>Department of Chemistry, School of Science, GITAM University, Hyderabad campus, Telangana, India

\*Corresponding author

### ABSTRACT

#### Keywords

Cu-Zn NPs ,  
Diclosulam,  
XRD, SEM,  
HPLC-UV, DT50

#### Article Info

Accepted:  
10 October 2020  
Available Online:  
10 November 2020

Copper doped Zinc Oxide nanoparticles (NPs) were prepared as a photo-catalyst by using a precipitation method for the removal of diclosulam pesticide in water. The experiment was performed under direct sunlight at a single fortification level (1 µg/ml) at different pH levels (pH 4.0, 7.0 and 9.0). The optimum catalyst concentration recommended for complete degradation was found as 100 mg/L under sunlight. Diclosulam residues in water were determined by HPLC- UV detector and the rate constant and DT50 values were calculated from the obtained data. Based on the results we observed that Cu-Zn NPs acted as excellent photocatalyst for the decontaminating of the diclosulam pesticide residues in water samples.

### Introduction

Diclosulam is an organic compound commercially available as a herbicide, with the chemical formula  $C_{13}H_{10}C_{12}FN_5O_3S$ . Diclosulam is a sulphonamide soil applied herbicide which controls broad-leaved weeds in peanuts, soybean and other crops. It is taken up by roots and foliage and inhibits the acetolactate synthesis [1]. It is used in non-cropland areas and for brush control. By entering the plant through the root zone and

moving throughout the plant, it works by interfering with photosynthesis [2]. Diclosulam, from the triazolopyrimidine sulfonanilide chemical family, is a selective herbicide recommended for the control of dicot weeds in soybean, which acts by inhibiting the enzyme acetolactate synthase (ALS) (Hanley and Billington, 2001) [3-5]. These materials are broad-spectrum herbicides used in the non-selective control of weeds and brushes in non-croplands and in the selective control of weeds in a limited

number of crops, such as citrus fruit and pineapple [6-8]. In order to ensure food safety, many nations, such as America, Canada, and Japan, have set the maximum residue limit (MRL) of diclosulam in foods as low as 0.03 ppm [9, 10]. Diclosulam is also found to be excellent in controlling perennial grasses. It is therefore necessary to establish sensitive methods for determining the concentration of diclosulam.

Photocatalysis is a term that dates back almost 100 years and could simply be defined as a change in the rate of chemical transformation under the action of light in the presence of a catalyst that absorbs light and is involved in a chemical reaction. Although examples of heterogeneous photocatalysis spanning this period can be found, a significant growth period in the field of photocatalysis took place in the 1970s.

The use of Cu-ZnO NPs as photocatalyst in visible light has already been reported to be effective in the photo degradation of various organic complexes. In this study, we have studied the effectiveness of Cu-ZnO NPs, which have been synthesized by a reaction of copper nitrate and zinc nitrate, for photo degradation of diclosulam in water under visible light.

Residues are quantified using a high-performance liquid chromatography UV method (HPLC-UV) to understand the pH effect with different pH water samples (4.0, 7.0 and 9.0). The optimum catalyst concentration required for complete residue decontamination has also been determined by varying the amount of the catalyst from 1 to 200 mg / L. The catalytic activity was measured at single concentration levels of the test item under direct sunlight.

X-Ray Diffraction (XRD), Scanning Electron Microscope (SEM), Transmission Electron Microscope (TEM) and Fourier Transform

Infra-Red (FTIR) spectroscopy have characterized the synthesized Cu-ZnO NPs.

## **Materials and Methods**

Reference analytical standard of diclosulam (purity 99 %), Zinc nitrate and Copper nitrate were obtained from Sigma Aldrich. The test item diclosulam 84% WDG was purchased from the local market. Acetonitrile, HPLC grade Water, Sodium hydroxide LR grade, Potassium chloride GR grade, Boric acid GR grade, Potassium biphthalate GR grade, Hydrochloric acid AR grade and Potassium phosphate AR grade were obtained from the Merck India limited. Distilled water was purified by using the Milli-Q Plus apparatus (Millipore, Bedford, MA, USA).

## **Preparation of Cu Doped ZnO nanoparticles**

Pure and Cu doped ZnO nanoparticles were synthesized by the Sol-gel process. 0.2 M aqueous ethanol solution of Zinc Nitrate was prepared under constant magnetic stirring of Zinc Nitrate for one hour. After complete dissolution of Zinc Nitrate, 0.1 M Copper Nitrate aqueous solution was added to Zinc Nitrate solution under high-speed constant stirring, drop by drop (slowly for 15 min) touching the walls of the vessel and adjusted to pH at 9 using 1.0 M NaOH. The mixed solution results in the formation of light blue precipitate and the stirring process again continued for 2 hours. The beaker sealed at this condition and allowed to settle overnight. The supernatant solution obtained separated carefully.

The remaining solution was centrifuged for 10 min and the precipitate obtained was centrifuged till no solvent remains. Thus, precipitated Cu-ZnO nanoparticles were cleaned repeatedly with deionized water to remove unwanted impurities bound with nanoparticles. The washed precipitate then

dried in an oven at about 60°C. During drying Cu-Zn(OH)<sub>2</sub> is completely converted into Cu doped ZnO.

### **Standard stock solution**

The reference standard stock solution was prepared by weighing accurately 10.25 mg of known purity diclosulam into a 10 ml volumetric flask using an analytical balance of 0.01 mg accuracy. The content of each flask was dissolved and makeup to the mark using HPLC grade acetonitrile.

### **Sample stock solution**

Accurately 23.67 mg of test item (purity 84.5%) of diclosulam was taken into a 20 mL volumetric flask. The content was dissolved, sonicated and makeup to the acetonitrile mark in 5 mL of acetonitrile. Consequently, the final concentration was 1000 mg/L. The stock sample solution was used for the preparation of dose samples in different aqueous solutions.

### **Acidic Buffer**

The buffer solution of pH 4.0 was prepared by dissolving 4.0 g of disodium hydrogen orthophosphate in 1.0 L milli-Q water and the pH was adjusted to 4.0 using 1.0 mole/L hydrochloric acid solution.

### **Neutral Buffer**

The buffer solution of pH 7.0 was prepared by dissolving 4.0 g of potassium dihydrogen orthophosphate in 1.0 L milli-Q water and the pH was adjusted to 7.0 using 1.0 mol/L sodium hydroxide solution.

### **Basic Buffer**

The buffer solution of pH 9.0 was prepared by dissolving 1.25 g of boric acid and in 1.0 L

milli-Q, water and the pH were adjusted to 7.0 using 1.0 mol/L sodium hydroxide solution.

### **Adsorption study of the catalyst**

Recovery studies in water and different pH waters were conducted with 100mg L<sup>-1</sup> level of catalyst and reported % of recoveries in distilled water and different pH water.

### **Method validation**

Validation of the method ensures the credibility of the analysis. The accuracy, precision, linearity and detection limit (LOD) and quantification (LOQ) parameters were considered in this study [11]. Recovery tests were used, samples spiked at concentration levels of 0.03 and 0.3 µg/mL to determine the accuracy. Different known concentrations (0.03, 0.1, 0.5, 1.0, 2.0 and 5.0 µg / mL) that were prepared by diluting the stock solution were used to determine linearity. The detection limit (LOD, µg/mL) was identified as the lowest concentration resulting in a 3-fold response to the baseline noise defined by the control sample analysis. The limit of quantification (LOQ, µg/mL) was established as the lowest concentration ration of a diclosulam with a 10-fold response to the baseline noise [12-13].

### **Photolytic and photocatalytic studies**

Photolytic and photocatalytic studies were carried out in a borosil glass bottle under sunlight at GITAM University, Visakhapatnam. Each one liter of milli-Q water, pH 4.0, 7.0 and 9.0 buffer solution were doped with 1 mL of 1000 mg/L stock solution of pesticide formulation to get 1µg/mL of active pesticide concentration. We prepared 2 sets, one set was used for photolytic study and another set used for the photo catalytic study. Before exposure to the

sunlight, the resultant suspension was sonicated in the dark for 10 min to get an even dispersion of Cu-ZnO NPs and attain adsorption equilibrium. Then the samples were exposed to direct sunlight. Aliquots of samples were collected on pre-determined intervals. The temperature of water samples during the period was 26 to 38°C. The samples collected on different sampling occasions were filtered using 0.2 µm PTFE membrane filter and collected the filtrates into amber-colored vials.

All the samples were stored in dark at <5°C before subjecting to HPLC-UV analysis. The samples fortified with Zn NPs particles were centrifuged using Beckman cooling centrifuge at 4000 rpm for 5 minutes at 5°C. Transferred the supernatant into the amber-colored bottles and stored in dark at < 5°C until analysis to avoid further degradation of residues.

### **Sampling**

Test samples were collected from the bottle at different depth on different time intervals after exposure to sunlight (0, 5, 10, 24 and 48 hours for the photo catalytic experiment). The collected samples were centrifuged and filtered through 0.2 µ filter and analyzed in HPLC.

### **Chromatographic separation**

The HPLC-UV system consisting of Shimadzu high-performance liquid chromatograph equipped with a reversed-phase Column Zorbex C8 (15cm length x 0.46 cm id x 3.5µm) was used in this study. The temperature of the oven was kept at 30°C.

The volume of the sample injected was 10 µL. Acetonitrile and HPLC water were mobile phases A and B [60:40 (v / v)]. The flow rate with a detector wavelength of 220 nm was

kept at 1.0 mL/min. For this analysis, the external standard calibration method was used.

## **Results and Discussion**

### **XRD Analysis**

Figure 1 represents the XRD spectra of pure and Cu doped ZnO nanoparticles synthesized using the sol-gel process. In figure 1 diffraction peaks appear at 12.78°, 16.78°, 29.29°, 31.38°, 35.40°, 36.40°, 38.86°, 39.27° and 45.25° respectively. Diffraction peaks keenly indexed as hexagonal wurtzite structure of ZnO. No change in the crystalline structure was detected due to Cu doping which suggests the majority of Cu atoms were in the ZnO wurtzite lattice. The average crystalline size and lattice strain calculated from the most intense peak of XRD spectra are found to be 23.8 nm and 0.0055 in the case of pure ZnO and 20.28 nm and 0.0071 nm in the case of Cu-doped ZnO nanopowders. From spectra, it is also clear that nanopowders of doped and undoped ZnO possess high crystallinity and purity. This shows that Cu<sup>2+</sup> ion successfully occupies the lattice site rather than the interstitial one. This is because the ionic radius of Cu<sup>2+</sup> (0.73Å) is very close to that of Zn<sup>2+</sup> (0.74Å), due to which Cu can easily penetrate the ZnO crystal lattice. From XRD data it was clear that the incorporation of Cu into ZnO lattice decreases the crystalline size, which further improves the structural properties of nanopowders.

### **SEM analysis**

The scanning electron microscopy (SEM) images of pure and Cu doped ZnO is shown in figure 2. The SEM micrograph indicates that, with increasing Cu concentration, the shape and morphology of ZnO nanoparticles change. The image revealed that the individual particles were composed of the

collection of particles of various shapes with increasing Cu concentration. This indicates that the morphology of ZnO nanoparticles is strongly affected by Cu ion doping. These images also show that with increasing Cu concentration and dispersivity, the agglomeration in nanoparticles increases, the homogeneity of particles was not good.

**FTIR analysis**

Figure 3 represents the FTIR spectra of pure and Cu doped nanoparticles recorded in the range of 400–4000 cm<sup>-1</sup>. The position and number of absorption bands depend not only on the structure of the crystal, the chemical composition, but also the morphology of the crystal. Fundamental modes of vibration observed around 3400 cm<sup>-1</sup> corresponds to OH vibrations. Peaks observed around 1600 cm<sup>-1</sup> corresponds to O-H-O vibrations. Significant modes of vibration of 1300 cm<sup>-1</sup> correspond to C-H stretching vibrations. It is very important to identify that Cu doping affects the spectra In Figure 3 the Zn-O band is observed at 455 cm<sup>-1</sup> and Figure 4 below 700 cm<sup>-1</sup> many peaks are observed attached

to Zn-O which assigned as a Cu-O stretching mode. This is due to the presence of Cu ion in the doped sample. A small hump observed at 2043.09 attributed to the presence of carbon dioxide. Various shifts observed in the spectra might be due to the Cu incorporation.

**TEM Analysis**

Figure 4 shows the TEM image of ZrO<sub>2</sub> NPs. The figure indicates that Cu-ZnO NPs were uniform and cylindrical. The average particle size calculated was about 50 nm using Image-J software.

**Specificity**

Specificity was confirmed by injecting the Mobile phase solvents i.e., Acetonitrile and HPLC water, sample solution standard solution and buffer controls (acidic, neutral, basic). The chromatograms did not have matrix peaks to interfere with the diclosulam residue analysis shown in Fig. 5, 6 and 7. Furthermore, the retention time of diclosulam was constant at 3.2 ± 0.4 min.

**Table.1** Calibration details of diclosulam

Concentration in (mg/L)	Peak area of diclosulam (mAU)
5	85247
2	33985
1	17025
0.5	8564
.1	1652
0.03	368

**Table.2** Statistical Parameters details diclosulam at 0.1 mg/L fortification level

Statistical Parameters (6 Replications)	Results
% of men Recovery	87.23
SD	1.61
% RSD	1.48
Horwitz Limit Value	1.52

**Table.3** Dissipation data for Photolytic decontamination of diclosulam in water under direct sunlight

Diclosulam			
Occasion (Days)	Residues (µg/mL)		
	pH 4.0	pH 7.0	pH 9.0
0	0.998	0.996	0.993
5	0.789	0.745	0.601
10	0.694	0.45	0.396
15	0.521	0.314	0.215
20	0.412	0.189	0.109
50	0.289	0.105	BDL
100	BDL	BDL	BDL

**Table.4** Dissipation data for photo catalytic decontamination of diclosulam in water under direct sunlight

Diclosulam			
Occasion (hours)	Residues (µg/mL)		
	pH 4.0	pH 7.0	pH 9.0
0	0.985	0.981	0.975
6	0.625	0.589	0.702
12	0.362	0.326	0.389
18	0.178	0.121	0.102
24	0.087	0.084	0.053
48	BDL	BDL	BDL

**Table.5** Kinetic parameters for Photolytic decontamination of diclosulam in water under direct sunlight

Kinetic parameters	Water		
	pH 4.0	pH 7.0	pH 9.0
Diclosulam			
DT <sub>50</sub> (Days)	28.87	15.70	6.36
k	-0.010	-0.019	-0.047

**Table.6** Kinetic parameters for photocatalytic decontamination of diclosulam in water under direct sunlight

Kinetic parameters	Water		
	pH 4.0	pH 7.0	pH 9.0
Diclosulam			
DT <sub>50</sub> (hours)	6.81	6.40	5.36
k	-0.044	-0.047	-0.056

**Fig.1** XRD spectra of copper doped ZnO nanoparticles

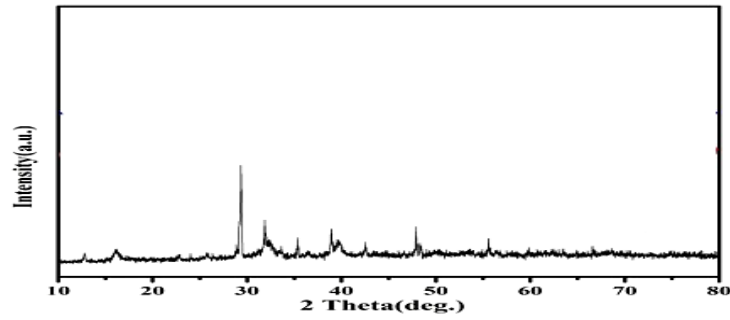


**Fig.2** SEM spectra of Cu doped ZnO NPs

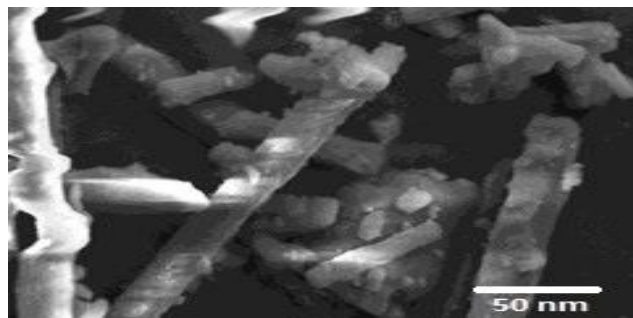


**Fig.3** FTIR spectra of Cu doped ZnO Nanoparticles

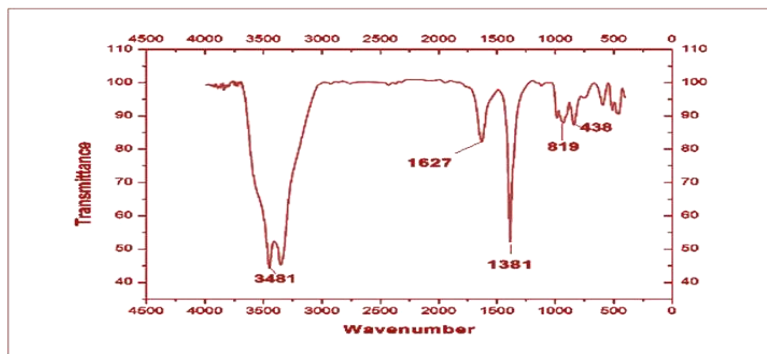


**Fig.4**

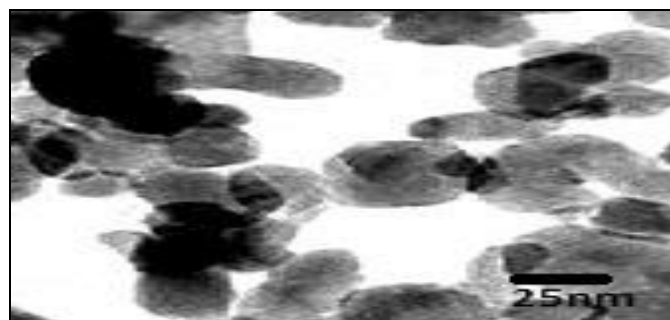


Fig.5 Representative chromatogram of diclosulam test item in acidic water- 12<sup>th</sup> hour

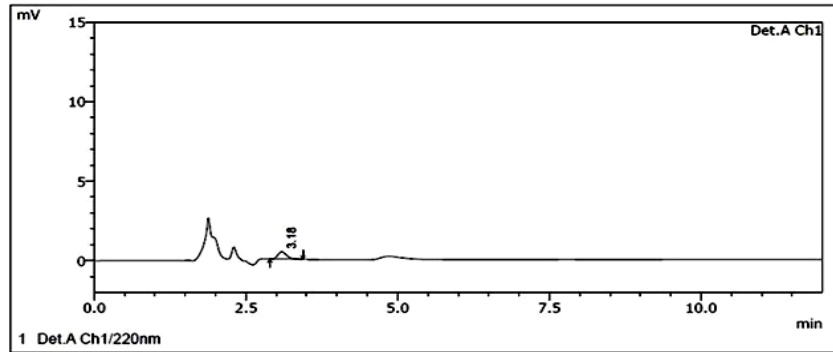


Fig.6 Representative chromatogram of diclosulam test item in neutral water -12<sup>th</sup> hour

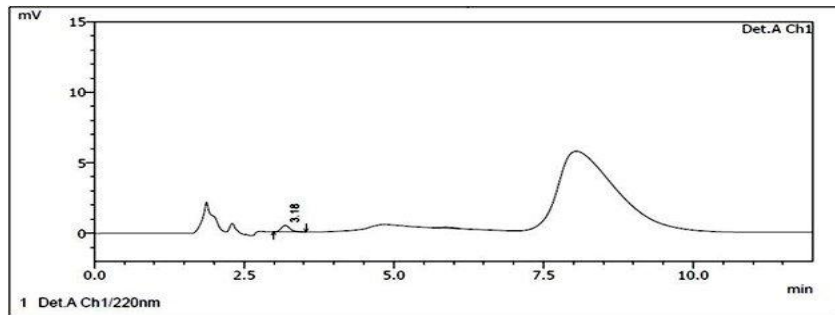


Fig.7 Representative chromatogram of diclosulam test item in basic water - 12<sup>th</sup> hour

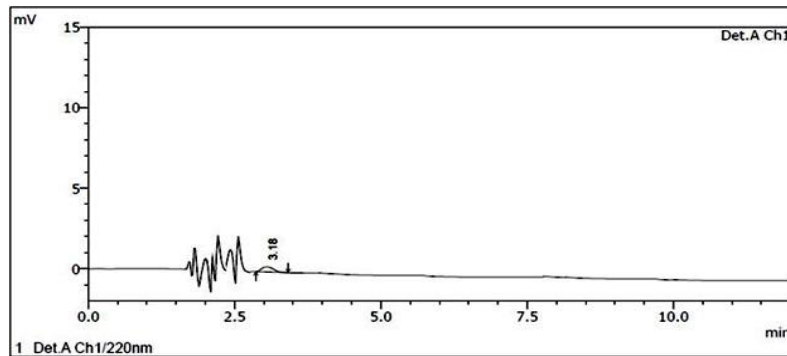
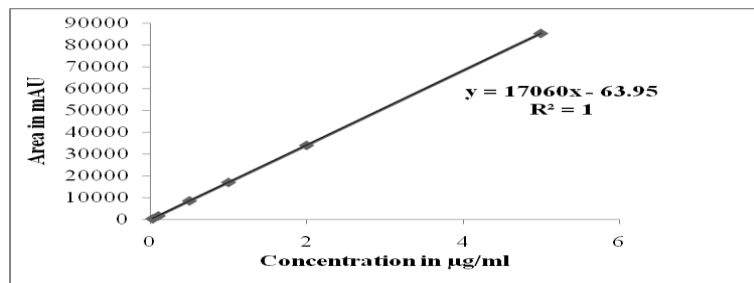
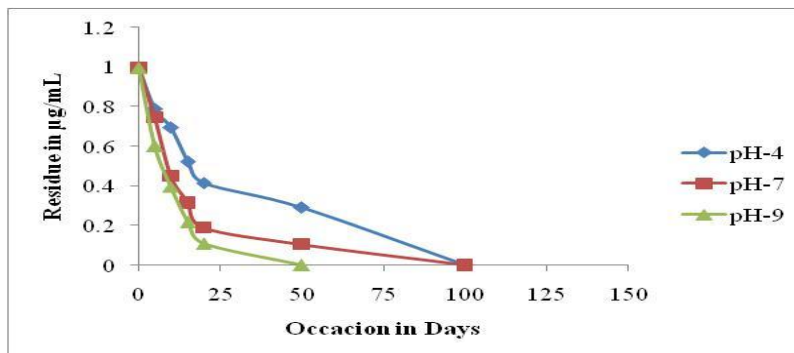


Fig.8 Representative Calibration curve of diclosulam standard

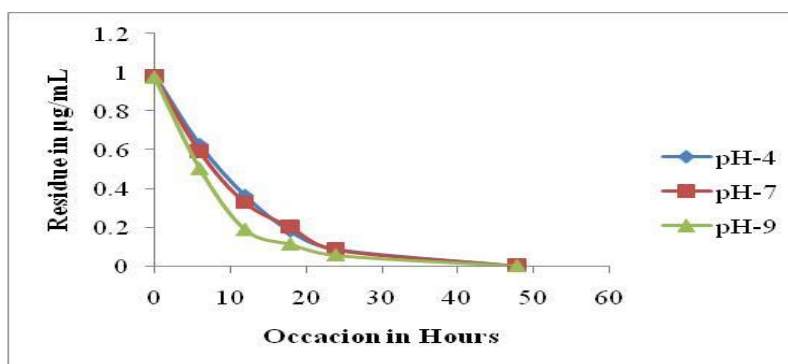




**Fig.9** Graph representing the dissipation curve of photolytic decontamination of diclosulam in water under direct sunlight



**Fig.10** Graph representing the dissipation curve of photo catalytic decontamination of diclosulam in water under direct sunlight



**Linearity**

Different known concentrations of diclosulam (0.03, 0.1, 0.5, 1.0, 2.0 and 5.0 µg/mL) were prepared into a different 10 mL volumetric flasks by diluting the stock solution. These standard solutions were directly injected into an HPLC. An analysis of six standard concentration solutions evaluated a calibration curve has plotted for the concentration of the standards injected versus area observed and the linearity of the method. The details were presented in Table 1. To calculate the linear regression equation, the peak areas obtained from various concentrations of standards were used. This was  $Y=15060X + 64.90$  with correlation coefficient of 0.9998 respectively. A calibration curve is shown in Fig. 8.

**Recovery**

The method had an acceptable recovery range (80 - 110 %) for pesticide in four different glasses of water. The Limit of Quantification (LOQ) was established as 0.03 mg/L from 10:1 peak to noise height ratio. Statistical parameters for recovery (0.03 mg/L). Table 2 presents the mean percentage of recovery, standard deviation (SD), percentage of relative standard deviation (percent RSD) and Horwitz Limit. The formula for calculation residue and statistical parameters are presented below the equitation.

$$\text{Residue content } (\mu\text{g/mL}) \quad (\text{Eq. 1})$$

Where A is the peak area of active content in the sample (µV\*sec); C is the concentration of

the standard solution ( $\mu\text{g/mL}$ ); and D is the peak area of active content in standard solution ( $\mu\text{V}\cdot\text{sec}$ ).

$$\text{Recovery \%} = \frac{\text{Recovered residue} \times 100}{\text{Fortified concentration}} \quad (\text{Eq. 2})$$

$$\% \text{ RSD} = \frac{\text{Standard deviation} \times 100}{\text{Mean}} \quad (\text{Eq. 3})$$

$$\text{Horwitz Limit} = 2^{-(1 - \log\sqrt{C})} \times 0.67 \quad (\text{Eq. 4})$$

Where C is the concentration

### **Adsorption study of the catalyst**

The amount of catalyst required for the decontamination was optimized as 100 mg/L for diclosulam, any further increase of catalyst had no significant effect on degradation. The adsorption of catalyst study was conducted by quantifying the concentration of diclosulam in water for three hours.

The recovery was 93 to 96%, 91 to 94%, 90 to 92% in acidic water, neutral water and basic water respectively. The results indicate no significant loss of residues due to adsorption. In the presence of the catalyst though, the dissipation was found rapid under sunlight.

### **Photolytic and photocatalytic study**

The photolytic degradation results of diclosulam in water showed the residues are highly stable, the stability decreased with decreasing pH. The results were shown in Table 3 and Fig. 9. Comparatively lower values of diclosulam in the presence of a catalyst (Photocatalytic) in different pH were recorded. The results were shown in Table 4 and Fig. 10.

The data demonstrate that the decontamination of diclosulam follows

pseudo-first-order kinetics in Cu-ZnO loaded water. DT50 values were calculated using the following formula: (Eq. 5).

Where 'k' is the slope of the curve obtained from the dissipation data.

For photolytic and photo catalytic studies, the calculated DT50 values are shown in Table 5 and Table 6. The constant value of the rate was calculated from the first-order rate equation by the linear regression equation. (Eq. 6)

Where dt is the time interval between t1 and t2 and a, x is at times t1 and t2 respectively the concentration of diclosulam. A plot of residue and rate concentration with R2 shows first-order kinetics in diclosulam dissipation. Diclosulam DT50 was calculated from the dissipation data by regression analysis.

The decontamination was fast when studied under sunlight in presence of Cu-ZnO. Due to the formation of electrons ( $e^-$ ) and positive hole ( $h^+$ ) in Cu-ZnO by absorbing energy from sunlight and the availability of electrons ( $e^-$ ) and the positive holes ( $h^+$ ) pairs contributing the simultaneous oxidation and reduction of diclosulam enhances the rate.

In conclusions the different water samples, the Cu-ZnO NPs were found to be an excellent decontaminating catalyst for diclosulam. In the absence of a catalyst, the compound persists for several days. Good separation and resolution were shown in the mobile phase, Acetonitrile and HPLC water, and the analysis time required for the chromatographic determination of three different types of buffers is very short (about 15 minutes for a chromatographic run).. Photo catalytic studies of diclosulam at various conditions such as acidic, basic and neutral reveals that the activity is enormously increased with Cu-ZnO NPs as the time frame

is fixed for a stipulated number of hours, whereas activity did not found without added Cu-ZnO NPs, even though experiments were carried out in several days.

## References

- Chaudhry, G. R.; Cortez, L. Degradation of Diclosulam by a *Pseudomonas* Sp. *Appl. Environ. Microbiol.* 1988, 54 (9), 2203–2207. <https://doi.org/10.1128/aem.54.9.2203-2207.1988>.
- Deepa, L.; Desai, B. K.; Latha, H. S. Research Article Biotoxic Effect of Diclosulam 84 % Wdg On Growth, Nodulation And Nitrogen Content Of Greengram. 2017, 9 (32), 4468–4470.
- De Souza, C. da C. B.; Borella, J.; Leal, J. F. L.; Tornisielo, V. L.; Pimpinato, R. F.; Monquero, P. A.; de Pinho, C. F. Limited Diclosulam Herbicide Uptake and Translocation-Induced Tolerance in *Crotalaria Juncea*. *Bull. Environ. Contam. Toxicol.* 2020, 104 (1), 114–120. <https://doi.org/10.1007/s00128-019-02742-7>.
- Donato, F. F.; Martins, M. L.; Munaretto, J. S.; Prestes, O. D.; Adaime, M. B.; Zanella, R. Development of a Multiresidue Method for Pesticide Analysis in Drinking Water by Solid Phase Extraction and Determination by Gas and Liquid Chromatography with Triple Quadrupole Tandem Mass Spectrometry. *J. Braz. Chem. Soc.* 2015, 26 (10), 2077–2087. <https://doi.org/10.5935/0103-5053.20150192>.
- Jakhar, R. R.; Sharma, R.; Singh, S. B. Evaluation of Diclosulam Residues in Soil at Harvest of Soybean. *Int. J. Curr. Microbiol. Appl. Sci.* 2017, 6 (2), 1459–1463. <https://doi.org/10.20546/ijcmas.2017.6.02.163>.
- Kumaravel S, P. R. A Reversed-Phase High-Performance Liquid Chromatography (RP-HPLC) Determination of Pesticide Residues in Tender Coconut Water (Elaneer/Nariyal Pani). *J. Chromatogr. Sep. Tech.* 2013, 04 (10), 4–6. <https://doi.org/10.4172/2157-7064.1000208>.
- Pareja, L.; Cesio, V.; Heinzen, H.; Fernández-Alba, A. R. Evaluation of Various QuEChERS Based Methods for the Analysis of Herbicides and Other Commonly Used Pesticides in Polished Rice by LC-MS/MS. *Talanta* 2011, 83 (5), 1613–1622. <https://doi.org/10.1016/j.talanta.2010.11.052>.
- QUEIROZ, S. C. N.; LAZOU, K.; SANDRA, P.; JARDIM, I. C. S. F. Determination of Pesticides in Water By Liquid Chromatography-(Electrospray Ionization)-Mass Spectrometry (Lc-Esi-Ms). *Pestic. Rev. Ecotoxicologia e Meio Ambient.* 2004, 14, 53–60. <https://doi.org/10.5380/pes.v14i0.3123>.
- Rajput, S.; Kumari, A.; Arora, S.; Kaur, R. Multi-Residue Pesticides Analysis in Water Samples Using Reverse Phase High-Performance Liquid Chromatography (RP-HPLC). *MethodsX* 2018, 5, 744–751. <https://doi.org/10.1016/j.mex.2018.07.005>.
- S, N.; N, R.; K, A. Comparative Evaluation of Extraction Procedures and Chromatographic Techniques for Analysis of Multiresidue Pesticides in Honey. *J. Environ. Toxicol. Stud.* 2017, 1 (1), 1–8. <https://doi.org/10.16966/2576-6430.102>.
- Singh, S. P.; Singh, V. P.; Nainwal, R. C.; Tripathi, N.; Kumar, A. Efficacy of Diclosulam on Weeds and Yield of Soybean. 2009, 41, 170–173.
- Velkoska-Markovska, L.; Petanovska-Ilievska, B.; Markovski, A. Application of High-Performance Liquid Chromatography to the Analysis of

Pesticide Residues in Apple Juice.  
*Contemp. Agric.*2018, 67 (1), 93–102.  
<https://doi.org/10.2478/contagri-2018-0014>.

Williams, R. M.; Kulick, A. R.; Yedlapalli, S.; Battistella, L.; Hajiran, C. J.; Sooter,

L. J. In Vitro Selection of a Single-Stranded Dna Molecular Recognition Element Specific for Diclosulam. *J. Nucleic Acids*2014, 2014, 1–9.  
<https://doi.org/10.1155/2014/102968>.

**How to cite this article:**

Varada Nageswara Rao, N. V. S. Venu Gopal and Patrudu, T. B. 2020. Removal of Diclosulam Pesticide Residues in Water samples using Cu Doped ZnO Nanocatalyst *Int.J.Curr.Microbiol.App.Sci.* 9(11): 910-921. doi: <https://doi.org/10.20546/ijcmas.2020.911.109>